23rd ABCM International Congress of Mechanical Engineering
December 6-11, 2015, Rio de Janeiro, RJ, Brazil

STUDY OF THE DRILLING PROCESS USED IN THE HOLE-DRILLING METHOD THROUGH THRUST FORCE MEASUREMENT AND TOOL WEAR ANALYSIS

Rodrigo Blödorn
Mariana Tiemi Tamura
Rodrigo Alberto Henke
Laboratório de Mecânica de Precisão (LMP), Laboratório de Metrologia e Automatização (LABMETRO) - Universidade Federal de Santa Catarina, Caixa Postal: 476 EMC, CEP: 88010-970 – Florianópolis, Santa Catarina
rbl@labmetro.ufsc.br, mtt@labmetro.ufsc.br, rah@labmetro.ufsc.br

Matias Roberto Viotti
Armando Albertazzi Gonçalves Júnior
Laboratório de Metrologia e Automatização (LABMETRO) - Universidade Federal de Santa Catarina,
Caixa Postal: 476 EMC, CEP: 88010-970 – Florianópolis, Santa Catarina
mov@labmetro.ufsc.br, a.albertazzi@ufsc.br

Rolf Bertrand Schroeter
Laboratório de Mecânica de Precisão (LMP) - Universidade Federal de Santa Catarina,
Caixa Postal: 476 EMC, CEP: 88010-970 – Florianópolis, Santa Catarina
rolf.schroeter@ufsc.br

Abstract. *This work presents a description of the procedure for measuring thrust force of a residual stress measurement equipment which combines a drilling module and an optical rosette for the application of the Hole-drilling Method (HDM). The drilling module consists of a high-speed pneumatic drill and a stepper motor for thrust. The main objective of this work is to characterize the overall behavior of the blind hole drilling process through the measurement of the thrust force and its correlation with tool wear. The results are qualitatively analysed from machining perspective. Two millimeters deep holes were produced in 20 steps of 100µm with an average rotational speed of 220,000rpm and two feed rates in three alloys: ASTM A36 steel, AISI304L stainless steel and AA6061 aluminum. In addition, dental inverted-cone end mills with known geometric parameters were used following recommendations from ASTM E 837-13a standard. SEM images were used to observe cutting tools wear. An increase in the overall force and vibration was noticed gradually with each additional step and micro-layered chips were formed. Furthermore, severe tool wear and extremely low cutting times along with peaks of thrust forces were observed.*

Keywords: *Blind hole, drilling, end mill, thrust force measurement, feed rate*

1. INTRODUCTION

Residual stresses correspond to the self-equilibrating stress state found within the bulk material in the absence of external loads. For this reason, their importance is often overlooked, but depending on the operational conditions a material is exposed to, such negligence can lead to the failure of the component. Residual stresses can bring beneficial or prejudicial effects to the material behavior depending on their sign and location, impacting significantly on material strength, fatigue life and dimensional stability (James, 1996; Macherauch, 1984; Schajer, 2013).

Many measurement techniques have been developed over the years to assess residual stresses either quantitatively or qualitatively; they vary in cost, complexity, time required to acquire data and suitability for a given measurement duty (Makino *et al.*, 2011). Among these methods, the Hole-drilling Method (HDM) constitutes a suitable and economical solution to in-field inspection of mechanical components during service life, since tolerable harm is introduced to the specimen and localized macroscopic residual stress can be measured (James, 1996; Viotti and Albertazzi, 2009).

The HDM is endorsed by the ASTM E837-13a standard (2013) and supply information about both uniform and non-uniform residual stress distributions. In short, the method consists of the drilling of a hole using a carbide inverted-cone dental end mill or small carbide end mills to relief residual stresses and induce a new equilibrium state, which results in strains on the reference surface that can be measured with strain gages or optical rosettes and then related to the initial stress state in the material. However, measurement results are sensitive to the hole geometry and machining induced residual stresses, since significant deviations from the standardized hole geometry and excessive plastic effects can lead to wrong stress values (Kapp, 2010; Rodacoski, 1997).

Despite the crucial relevance of the drilling process for an accurate and reliable application of the HDM, little attention has been paid to the machining aspects. This work investigates the thrust forces exerted during the hole drilling using the residual stress measurement device developed at LABMETRO/UFSC. Results were analysed qualitatively due the available measurement procedure, instability of the process and apparent unrepeatability of the data.

2. RESIDUAL STRESS MEASUREMENT BY THE HOLE-DRILLING METHOD

The HDM for residual stress measurement predicts a perfectly cylindrical flat-bottomed hole, orthogonal to the drilled surface. The closer to this geometry specification, the better the model will represent the hole. Numerical coefficients are introduced in the formulation to correct the model when the hole drilled to account to plastic effects (ASTM E 837-13a, 2013).

Residual stresses are introduced into the workpiece by the drilling process; some material transformations can evidence the presence of machining induced residual stress through the plastic deformation of the material in the drilled zone, hardening of the hole walls and increase in microstructural defects. The plasticised layer thickness is primarily influenced by the following factors: cutting force; temperature gradient; geometry; properties; tool sharpness and wear; workpiece material and material removal rate. The plastic deformation in the surrounding region of the hole edge has influence in the results of the measurement, since the linear formulation becomes invalid in the analysis of this region (Rodacoski, 1997; Kapp, 2010).

According to the literature, the absolute value of the residual stress near to the surface is high and continuously decreases as the depth from the machined surface increases. The residual stress can be tractive or compressive, and the affected layer can be shallow or deep, depending on the work and material conditions, as well as on tool geometry. Compressive residual stresses can be present at the surface and tractive stresses right below the surface or vice-versa (El-Axir, 2002; Davim, 2010; El-Khabeery and Fattou, 1989).

Manual drills were used when this residual stress measurement method was created, as in the pioneering work of Mathar in 1934. However, cutting speeds increased along the years and the use of high speed dental turbines became very common since 1980. Another challenge is the residual stress measurement in materials of high hardness, as ceramics and some steel alloys, as even carbide tools rapidly lose sharpness during the machining, introducing considerable stress levels in the workpiece and therefore increasing the measurement uncertainty (Rodacoski, 1997).

2.1 Machining forces during drilling

Drilling is defined as a machining process with a circular cutting movement. The drilling tool has a feed direction parallel to its rotational axis that maintains its relative positioned to the workpiece (Zeilmann, 2003). According to DIN 6580, the cutting speed v_c of the drilling process is related to the tool angular velocity (w), being proportional to the tool radius, where its maximum value is reached on the tool edge (Fig. 1a).

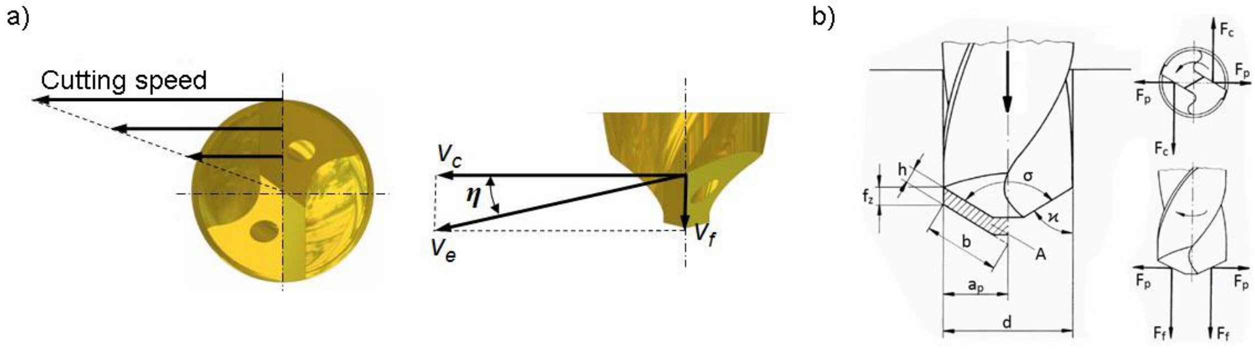

Figure 1. Speeds (a) and forces (b) during the drilling process (adapted from Boeira, 2010 and Paucksch, 1996).

In the drilling process, each cutting edge of the tool describes a circular trajectory around its rotational axis, with the same feed per tooth f_z. This tools feed movement together with the cutting depth (Fig. 1b) form the chip area per tooth (A), that is directly related to the machining forces (Paucksch, 1996).

3. EXPERIMENTAL PROCEDURE

Force signals were measured with a dynamometer, which utilizes piezoelectric crystals that transform the applied mechanical stress in electric charges. These charges were then amplified with a Kistler 5011B charge amplifier and the acquisition was made with a NI USB-6008 acquisition board. The dynamometer and charge amplifier are recommended to dynamic charges due to the nature of the piezoelectric crystal phenomena and to the lack of a drift compensation in the charge amplifier. For the signal conditioning, visualization and recording of the data the software LABVIEW was used. Figure 2 exemplifies the order in which the signal was acquired.

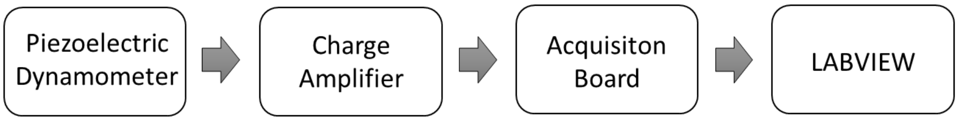

Figure 2. Flowchart of the signal.

The cutting tools currently used in the drilling of blind holes are dental end mills, with an inverted-cone geometry. The shank is made of high-speed steel (HSS) and the body of tungsten carbide, based on WC-Co, as seen at the bottom of Figure 3, without coating. The tool has a diameter of 1.6mm, a tapered angle of 84.5º and six cutting edges.

Along the cutting edge of the end mill the flank angle γ was 28±3°, the rake angle α 2±2° and the cutting edge radius ρ 6±3µm. Close to the center (r=0.15mm), the rake angle α was -10±2° and the flank angle γ 28±3°. In the region of the chamfer, the rake angle was practically the same as that for the rest of the cutting edge, but the flank angle γ decreased to 15±3°.

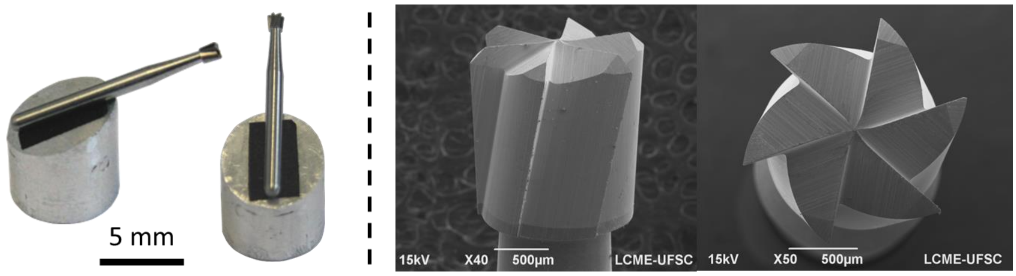

Figure 3. Dental end mill used in the experiment (Blödorn, 2014).

The specimens were acquired as flat sheets with thicknesses of 6.30mm, 6.35mm and 12.00mm for the A36 steel, AISI 304L stainless steel and AA6061 aluminum alloy, respectively. These sheets were cut into the final dimensions of 135mm x 25mm and submitted to heat treatment to eliminate any residual stresses.

The residual stress measurement device used in the tests (Fig. 4) consists of a pneumatic drill and an ESPI interferometer with radial in-plane sensitivity. The pressure supplied to the turbine was kept at 0.3MPa (3 bar) during all the tests. However, since the turbine does not provide a constant torque during the process, a variation of the rotational speed (which was around 220,000rpm) was observed according to the machinability of the material. The only machining parameter varied during the test was the feed rate (v_f=0.20mm/min and v_f=0.40mm/min). Thus, the feed per tooth were f_z=1.5x10^{-7}mm and f_z=3.0x10^{-7}mm, respectively. Comparing these values to the edge radius, the edge radius is 40,000 and 20,000 times greater than the feed per tooth for the first and second cases respectively.

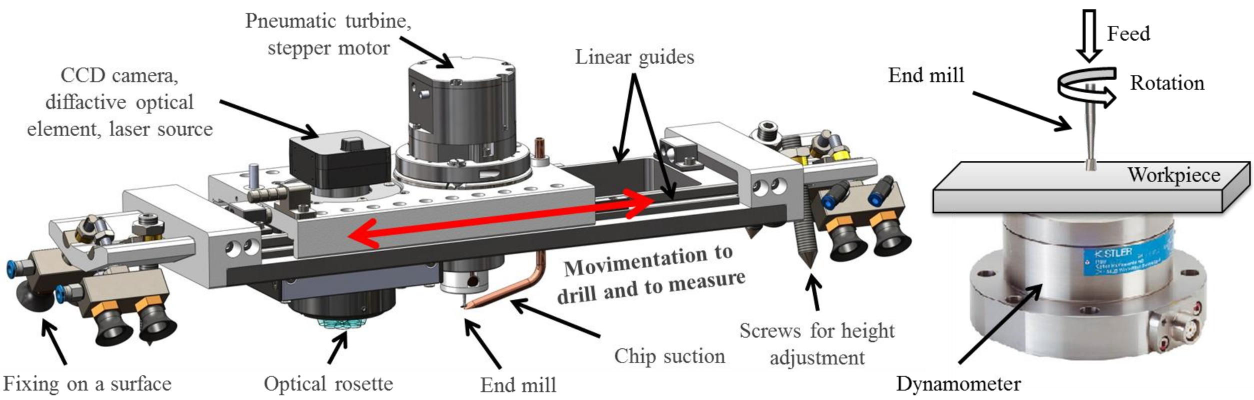

Figure 4. Equipment for residual stress measurement and dynamometer.

The stepper motor is responsible for the feed dynamics, which means this equipment has a major influence on the thrust force. For this reason, an understanding of how the steps are provided is necessary. Each complete step has a linear displacement of 12.7μm. However, it is possible to divide this step in a half, a quarter or one eighth of a full step with a driver for a better control of the feed rate. So the two feed rates could be achieved by determining the ratio in which the full step is divided and the signal frequency sent by the driver to the stepper motor.

In this work, the one-quarter ratio was chosen and the expected linear displacement for each minor step would be 3.17μm. To verify this displacement, a dial gauge was positioned on the edge of the stepper motor so the real linear displacement could be measured. It was found that the minor steps have irregular values, but a pattern was observed. The first three minor steps have values in the order of approximately 1.0μm to 1.5μm and the fourth minor step showed a bigger displacement of 9μm. Although the minor steps were not constant, the sum of the four minor steps displacements was equal to 12.7μm, which is the original undivided value of the stepper motor linear displacement per step.

These minor linear displacements measured most likely do not correspond to the real displacement of the drilling process, for there are several others variables that were not considered in this verification. On the other hand, they are a guideline to analyse the signal.

The final hole depth was 2mm, drilled in 20 steps of 100μm each. All drilling tests were performed without the use of coolant or lubricant fluids and it was established that each hole must be drilled by a new end mill.

4. RESULTS

In Figure 5a a representative thrust force of the process is shown. At first, it seems that the signal measured is only the vibration of the drilling process. This hypothesis was refuted by calculating the mean value of the thrust forces per step measured and it showed they were greater than zero. Therefore, part of the signals measured may represent the thrust force. These mean values also did not show any observable tendency, which is an indicator that the process is extremely complicated and cannot be analysed quantitatively.

When the variation of the rotational speed occurs (lower frequency), the cutting process happens and the peaklike signals appeared. Figure 5b and Figure 5c exemplify the huge amount of thrust force information gathered during the process due to the high rotational speed.

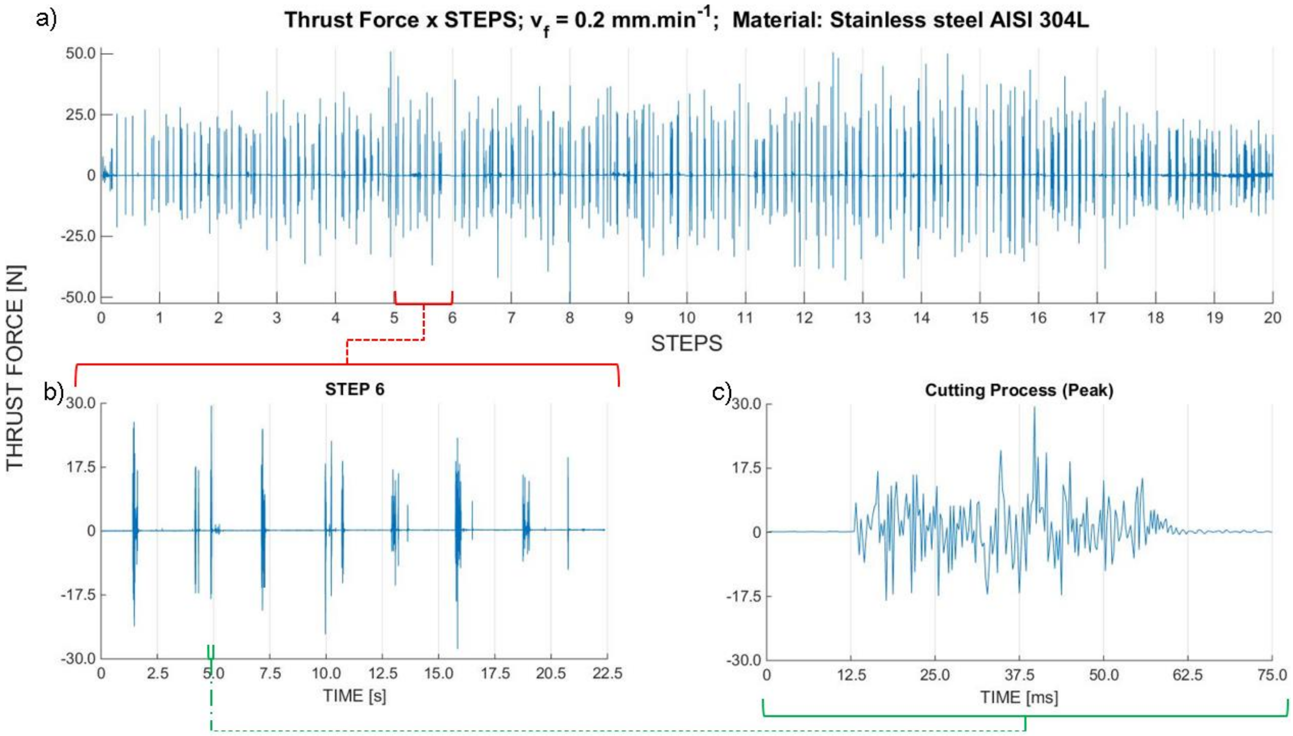

Figure 5. Thrust force in different time frames.

The rotational speed frequency during the cutting process is approximately 3.7kHz (220,000rpm), the tool also has six cutting edges which influence differently on the thrust force. In order to acquire *n* points for each rotation of a single tool cutting edge it would demand a sampling rate of *n* times 22.2kHz. Additionally, the acquisition board could not support this frequency and the sampling rate utilized was 4kHz; in other words, every complete rotation given by the tool would be represented by one point in the measured data. Comparing the given sampling rate with the frequency in which the stepper motor advances for the two feed rates (v_f= 0.20mm/min and v_f=0.40mm/min), respectively 3,800 and 1,900 points would be acquired each time the stepper motor advances.

Figure 5c shows that the thrust force repeatedly inverts its signal and negative thrust forces were measured in the process. Negative thrust forces measured could be also explained by the low rigidity of the tool holder. Low rigidity in the feed direction implies that the bearing may be acting as a spring with the process alternating between the three possibilities shown in Figure 6; this phenomenon could be a reaction of the workpiece material pushing the tool upwards when the minimum chip thickness is not reached, as a rubbed material protrusion could be formed and elastically deformed without cutting during the tool revolution between feed steps. The frequency of the signal inversion was calculated and it ranged from 1.7kHz to 2.1kHz, which is closer to the rotation frequency than the other movements.

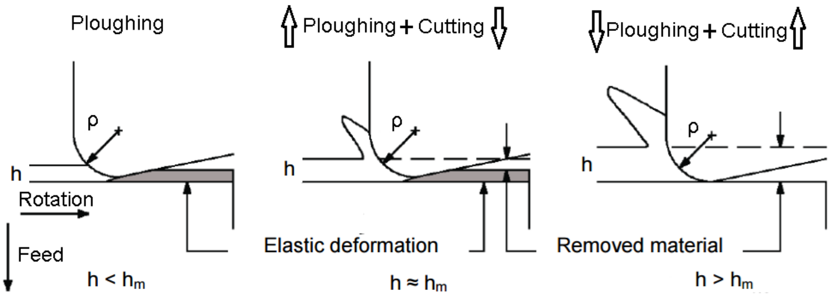

Figure 6. Microcutting mechanisms (adapted from Chae, Park and Freiheit, 2006).

Measuring conditions were not optimal and little information about the real thrust force value could be extracted. On the other hand, some patterns in the thrust force during the hole drilling were observed for all materials and feed rates which could mean that they are inherent to the process. The cutting process is not continuous since the peaks of thrust force appear distant from each other because of the alternate cycles of metal cutting and rubbing. In the first two steps, the overall thrust force is smaller due to the incipient friction between the tool and the hole wall.

When increasing the steps in the hole drilling process the cutting time also increased (longer wave trains). At the beginning the cutting times are very short and the distinction between the linear displacements of the stepper motor is possible. In an intermediate step of the hole, Fig. 7b, the cutting times are longer and the number of peaks increase. The last step, Fig. 7c, presents a denser graphic with longer cutting times and peaks blended together, indicating that the tool and the material remain in contact for longer times, since the loss of tool sharpness worsens the machining process.

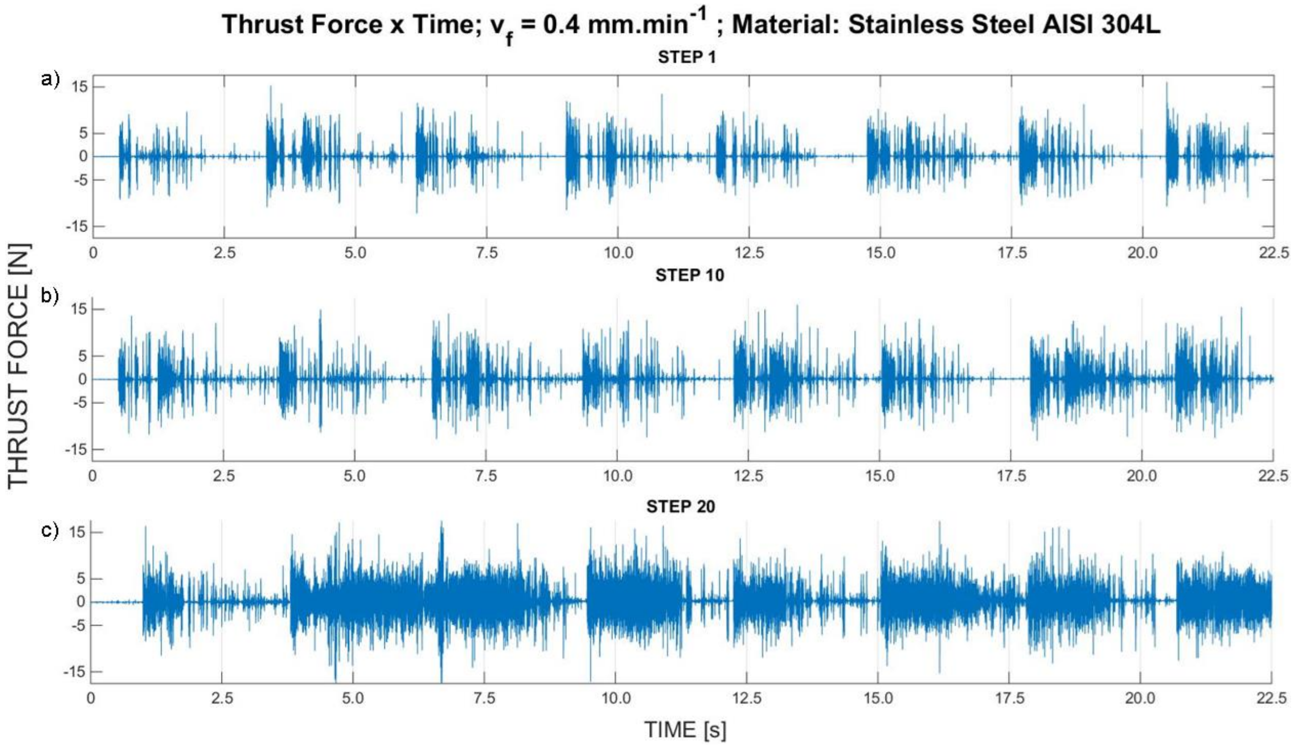

Figure 7. Thrust force for increasing hole depths; a) 0 to 100μm; b) 1000 to 1100μm; c) 1900 to 2000μm.

During the experiments, in more than half of the holes produced, tool chipping and breakage were observed (Figure 8). Furthermore, new or barely used tools also broke with no apparent warning. A low rigidity on the bearing of the tool would give the tools mobility on the hole plane and therefore explain these several breakages. Grant *et al.* (2002) already discussed that some disadvantages of combination of high speed air turbine and the dental tungsten-carbide inverted-cone end mill: the end mill can be damaged before the conclusion of the first hole; very high speeds are associated to low torques, which can lead to the drill stalling and sticking; and finally, the backlash in the closely spaced bearings that can provoke significant uncertainties concerning the cutting edge location. The data acquired during the holes in which the tools presented catastrophic failure were not used in the previous analyses.

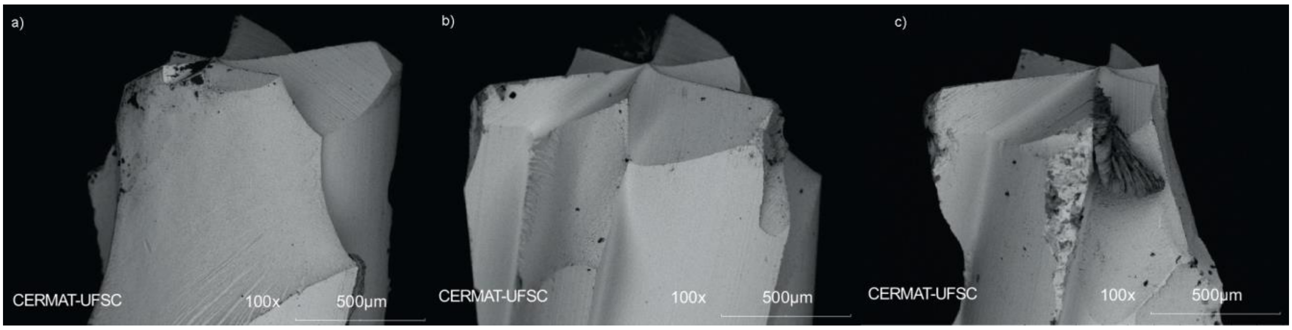

Figure 8. Broken end mills; a) v_f = 0.40mm/min, Material: AISI 304L; b) v_f = 0.20mm/min, Material: AISI 304L c) v_f = 0.20mm/min, Material: A36.

The A36 steel alloy was the only material in which a tool was able to perform two subsequent holes without breaking so the toolwear evolution could be noticed. The AISI 304L stainless steel demonstrated the highest thrust force of the experiments and faster cutting times. The AA6061 aluminum alloy is very ductile and combined with severe plastic deformation and heat generation smeared the alloy in the tools cutting faces. This precluded the tools ability to cut and a second hole was not attempted. Figure 9 shows an image taken after the hole was drilled for each material and feed rate.

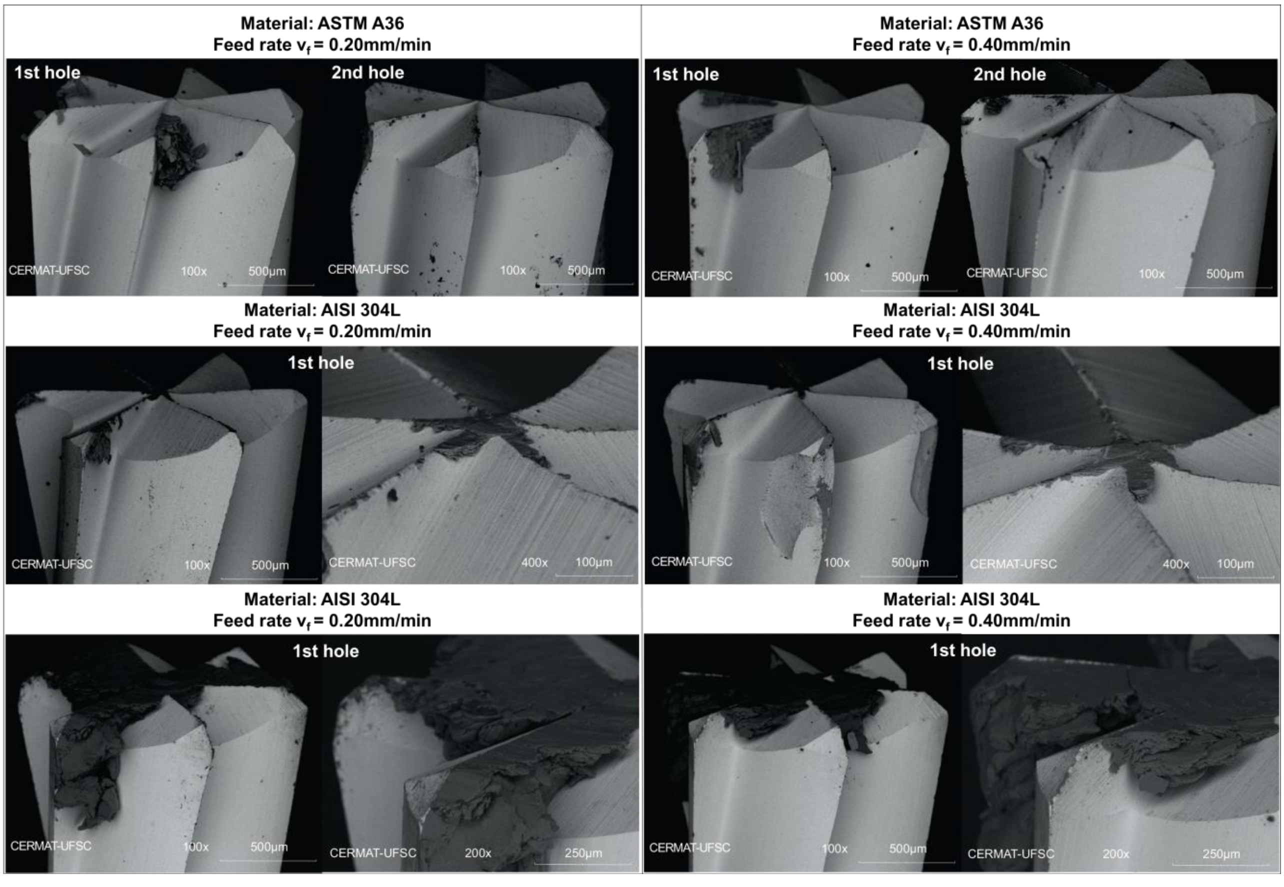

Figure 9. End mills after the hole was drilled.

The minimum chip thickness is often between 5% and 38% of the tool edge radius (Filiz *et al.,* 2007). The feed per tooth is 20,000 to 40,000 smaller than the tool edge radius. The consequence of this is a large negative rake angle, which makes the process dominated more by rubbing and compression instead of by cutting (Lee and Dornfel, 2002). Figure 10 shows that chip formation exists and its thickness is very close to the minimum chip thickness.

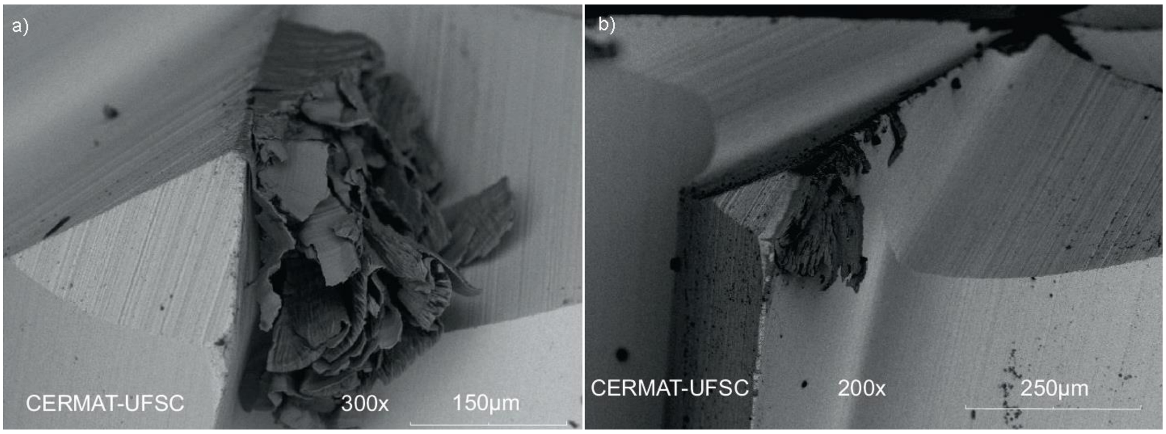

Figure 10. Chip formed in the process; a) v_f = 0.2mm/min, Material: A36; b) v_f = 0.2mm/min, Material: AISI 304L.

An estimation of the chip thickness produced can be derived from Fig. 10. Then, it is possible with some approximations to utilize Kienzle's equation (1) for determining a range of specific cutting forces for this process. Although the chip thickness is small and a micromachining model would be more suited. The values assumed were:

a) Chip width (b) is 80% of the total length of the cutting edges, assuming the tools center acts like an indentation;
b) Chip thickness is 1μm (h_{ch});
c) Uncut chip thickness (h) depends on the chip compression ratio (2) that varies from 1.2 to 4.0 in common materials, since the chip thickness estimated suffered deformation (König and Klocke, 2002);
d) Kienzle's exponent (m_f) varies between 0.1 and 0.3 in common materials;
e) Thrust force is the maximum reached in the process.

$$F_f = k_{f1.1}.b.h^{1-m_f} \tag{1}$$

$$\Lambda_{ch} = h_{ch}/h \tag{2}$$

Table 1 indicates the maximum thrust force reached for the three materials and feed rates, the step when it occurred and a range for the specific cutting force calculated. The maximum value of the thrust force appeared randomly in the hole drilling process. A decrease in overall thrust force was noted for the higher feed.

Table 1. Maximum thrust force and estimated specific thrust force.

	ASTM A36		AISI 304L		AA6061	
Feed rate [mm/min]	0.20	0.40	0.20	0.40	0.20	0.40
Maximum thrust force [N]	36.7	28.8	51.0	26.2	40.5	35.6
Step	19th	3rd	6th	20th	12th	8th
k_f [kN/mm^2]	1.4~16.7	1.1~13.1	2.1~23.0	0.9~11.9	1.5~18.4	1.3~16.2

5. CONCLUSIONS

This paper studied the drilling process of an equipment used for residual stress measurements, which utilizes the HDM, by analysing the thrust force and SEM images of the tool. Feed rate is intermittent and irregular due to the stepper motor dynamics meaning the real feed rate of the process is unknown. Feed steps do not always reach the minimum chip thickness and material ploughing occurs. The data measured may not be an accurate representation of the real thrust force due to the high rotation frequency, in consequence, the dynamometer and acquisition board may not be adequate for this process. Denser signals mean higher interaction times between the tool and the workpiece, therefore, a worse cutting process. Frequent and unpredictable tool breakage indicates an unstable process. This instability may be linked to the low rigidity of the tool bearing which also explains the constant thrust force signal inversion.

6. ACKNOWLEDGEMENTS

The support of PETROBRAS, PIBIC/CNPq, CERMAT, LCME, LABMETRO and LMP are gratefully acknowledged.

7. REFERENCES

American Society for Testing and Material. ASTM E 837.13a, 2013. *Standard Test Method for Determining Residual Stresses by the Hole-Drilling Strain-Gage Method*. West Conshohocken.

Blödorn, R., 2014. *Estudo do Furo e Processo de Furação Empregado no Método do Furo Cego para Medição de Tensões Residuais*. Master thesis, Universidade Federal de Santa Catarina, Florianópolis.

Boeira, A.M.G., 2010. *Modelagem e Simulação das Forças na Furação com Brocas Helicoidais a Partir de Dados Obtidos no Torneamento de Segmentos Cilíndricos*. Ph.D. thesis, Universidade Federal de Santa Catarina, Florianópolis.

Chae, J., Park, S.S., Freiheit, T., 2006. "Investigation of micro-cutting operations". In: *Int. J Machine Tools and Manufacture*, Vol. 45, p. 313-332.

Davim, J.P., 2010. *Surface Integrity in Machining*. Springer, Berlin.

DIN 6580., 1985. *Begriffe der Zerspantechnik: Bewegungen und Geometrie des Zerspanvorganges*. Beuth Verlag GmbH, Berlin, Germany.

El-Axir, M.H., 2002. "A method of modeling residual stress distribution in turning for different materials". In: *International Journal of Machine Tools and Manufacture*, Vol. 42, p. 1055-1063.

El-Khabeery, M.M and Fattouh, M., 1989. "Residual stress distribution caused by milling". In: *International Journal of Machine Tools and Manufacture*, Vol. 29, p. 391-401.

Filiz, S., Conley, C.M., Wasserman, M.B., Ozdoganlar, O.B., 2007. "An experimental in vestigation of micro-machinability of copper 101 using tungsten carbide microendmills". In: *Int. J. Machine Tools and Manufacture*, Vol. 47, p. 1088-1100.

Grant, P.V, Lord, J.D., Whitehead, P.S., 2002. *Measurement Good Practice Guide No. 53 - Issue 2: The Measurement of Residual Stresses by the Incremental Hole Drilling Technique*. Crown, Middlesex, UK.

James, M. R., 1996. "Introduction". In *Handbook of Measurement of Residual Stresses*. Fairmont Press. p. 1–4.

Kapp, W.A., 2010. *Desenvolvimento de uma roseta óptica difrativa para medição de deslocamentos, deformações, tensões mecânicas e tensões residuais mecânicas*. Ph.D thesis, Universidade Federal de Santa Catarina, Florianópolis.

König, W. and Klocke, F., 2002. *Fertigungsverfahren 1: Drehen, Fräsen, Bohren*. Springer-Verlag Berlin Heidelberg, Aachen, Germany.

Lee, K. and Dornfel, D., 2002. "An experimental study on burr formation in micro-milling aluminum and copper". In: *Trans. North American Manufacturing Research Institute*, Vol. 30, p. 255-262.

Macherauch, E., 1984. "Residual Stresses". In: *Application of Fracture Mechanics to Materials and Structures*, p. 157–192.

Makino, A., Nelson, D.V., Hill, M.R., 2011. "Hole-Within-a-Hole Method for Determining Residual Stresses". In: *Journal of Engineering Materials and Technology*, Vol. 133, p. 201–208.

Mathar, J., 1934. "Determination of initial stresses by measuring the deformation around drilled holes". In: *Trans. ASME*, Vol. 56, p. 249–254.

Paucksch, E., 1996. *Zerspantechnik.* Vieweg Verlag, Germany.

Rodacoski, M.R., 1997. *Medição de tensões residuais com holografia eletrônica*. Ph.D thesis, Universidade Federal de Santa Catarina, Florianópolis.

Schajer, G. S., 2013. *Practical Residual Stress Measurement Methods*. Wiley.

Viotti, M. R. and Albertazzi Jr., A.G., 2009. "Industrial Inspections by Speckle Interferometry: General Requirements and a Case Study". In *SPIE Europe Optical Metrology. International Society for Optics and Photonics*, Vol. 7389, p. 73890G1-73890G15.

Zeilmann, R.P., 2003. *Furação da Liga de Titânio TiAl6V4 com Mínimas Quantidades de Fluido de Corte*. Ph.D. thesis, Universidade Federal de Santa Catarina, Florianópolis.

8. RESPONSIBILITY NOTICE

The authors are the only responsible for the printed material included in this paper.